Canted antiferromagnetic ground state in $Sr_3Ir_2O_7$

Canted antiferromagnetic ground state in $Sr_3Ir_2O_7$

I Nagai[1,2], Y Yoshida[1,2], S I Ikeda[2], H Matsuhata[2], H Kito[2] and M Kosaka[3]

[1] Japan Society for the Promotion of Science, Chiyoda, Tokyo 102-8471, Japan
[2] Nanoelectronics Research Institute AIST, Tsukuba, Ibaraki 305-8568, Japan
[3] Faculty of Science, Saitama University, Saitama 305-8568, Japan

E-mail: nagai-ichi@aist.go.jp

Abstract

We have characterized the ground state of $Sr_3Ir_2O_7$ by performing measurements of electrical resistivity, magnetic susceptibility, magnetization, specific heat and electron diffraction (ED). Polycrystalline samples of $Sr_3Ir_2O_7$ have been synthesized by using a high-pressure technique. $Sr_3Ir_2O_7$ exhibits weak ferromagnetism with a small ferromagnetic component (2×10^{-3} μ_B/Ir) below $T_C \sim 280$ K. The temperature dependence of the electrical resistivity ρ shows semiconducting-like behaviour; $d\rho/dT < 0$ with an anomaly near T_C. From the result for specific heat, a λ-type anomaly appears at T_C, indicating a second-order phase transition. The ED patterns below and above T_C imply that there is no evidence of structural phase transition at T_C with substantial symmetry change. These experimental results exclude the possibility of ferromagnetic ordering with extremely small magnetic moments below T_C. Taking into account that certain pairs of Ir^{4+} ions lose the centre of inversion, this leads to the conclusion that the weak ferromagnetism is derived from canted antiferromagnetism.

1. Introduction

Ruddlesden–Popper (RP)-type oxides including a 4d or 5d transition metal have been paid attention since the discovery of high-T_C superconductivity in $(La, Ba)_2CuO_4$ [1]. Recently, the physical properties and structural analysis of an RP-type ruthenate $Sr_3Ru_2O_7$ have been investigated [2–13]. $Sr_3Ru_2O_7$ has a double-layered perovskite structure with RuO_6 octahedra rotated [2, 3]. The rotation angle was reported to be $\sim 7°$ [3]. It has been confirmed that the RuO_6 octahedral rotations were ordered normal to the RuO_2 plane [3]. This bilayered ruthenate did not exhibit superconductivity [4–8] despite its quasi-two-dimensional metal state [8], analogous to single-layered Sr_2RuO_4 [14]. The temperature dependences of susceptibility for polycrystalline [4, 5] and single-crystalline [8] $Sr_3Ru_2O_7$ showed a maximum around 16 K. This phenomenon was interpreted as enhanced paramagnetism [8], because there was

no evidence for any static long-range order from the experimental results for specific heat, nuclear magnetic resonance (NMR) or neutron scattering [2, 13].

Several papers on RP-type iridates, Sr_2IrO_4 [15–19], $SrIrO_3$ [20] and $Sr_3Ir_2O_7$ [21–25], have been reported. Polycrystalline samples of single-layered perovskite Sr_2IrO_4 reveal weak ferromagnetism below $T_C = 240$ K, which is likely to come from canted antiferromagnetism [15]. However, the existence of the canted antiferromagnetism has not been confirmed directly. Moreover, it has not been investigated whether the magnetic ordering accompanies structural transition or not. A metal–nonmetal transition occurs for a current along the in-plane and out-of-plane directions at $\sim$120 K in single-crystalline Sr_2IrO_4 grown by a flux method [16], while polycrystalline Sr_2IrO_4 shows semiconducting behaviour in the temperature range 50–300 K [17, 18]. No corresponding anomaly was seen in the electrical resistivity at T_C in either the single-crystalline [16] or polycrystalline samples [17, 18].

Double-layered perovskite $Sr_3Ir_2O_7$ has a similar crystal structure to $Sr_3Ru_2O_7$ [21, 22]. It was reported that the IrO_6 octahedra also rotate by $\sim$12° around the c-axis, normal to the IrO_2 plane, as observed in Sr_2IrO_4. The amount of IrO_6 rotation angle for $Sr_3Ir_2O_7$ is nearly the same as that for Sr_2IrO_4. Very recently, Cao *et al* reported the transport and magnetic properties of single-crystalline $Sr_3Ir_2O_7$ grown by a flux method [23]. They remarked that the single-crystalline $Sr_3Ir_2O_7$ was a ferromagnetic insulator below $T_C = 285$ K. The resistivities along all the principal axes increased rapidly with decreasing temperature below T_C. This single-crystalline $Sr_3Ir_2O_7$ exhibited an unusual temperature dependence of magnetization for $\mu_0 H < 0.2$ T, in which the magnetization became negative below 20 K under a field cooling sequence.

In this study, we focus on RP-type $Sr_3Ir_2O_7$ for the following reason. Even the natures of the magnetic susceptibility and electrical resistivity for $Sr_3Ir_2O_7$ have not been understood enough, as described above. In particular, the magnetic ground state has not been confirmed yet. It is worthwhile confirming the magnetic ground state of $Sr_3Ir_2O_7$ to assist us in understanding the physical properties of $Sr_{n+1}Ir_nO_{3n+1}$ systematically. Specific heat and ED measurements give us important information about the phase transition at T_C. In this paper, we report the sample preparation, magnetization, electrical resistivity, specific heat, and ED for polycrystalline $Sr_3Ir_2O_7$ in order to discuss the magnetic ground state.

2. Experimental details

Polycrystalline samples of $Sr_3Ir_2O_7$ were synthesized by using a high-pressure technique as follows. First, the precursors of $Sr_3Ir_2O_7$ were prepared from $SrCO_3$ and IrO_2 with nominal compositions of $Sr_3Ir_2O_7$. These materials were mixed and heated at 1173 K for 12 h in air. Second, the precursors were then placed in gold capsules and pressed up to 2 GPa using a cubic-anvil-type high-pressure apparatus at room temperature (RT). Then, the temperature was increased up to 1273 K, held constant for 2 h, and finally dropped down to RT. We characterized the obtained samples at RT by powder x-ray diffraction with Cu Kα radiation. Figure 1 shows an x-ray powder diffraction pattern for $Sr_3Ir_2O_7$. The arrowed peaks correspond to those of $SrIrO_3$. The samples were found to be almost single phase except for containing a tiny amount of impurity $SrIrO_3$. We have performed preliminary experiments in order to estimate a value of the fraction of this second-phase $SrIrO_3$. A polycrystalline sample of single-phase $SrIrO_3$ was synthesized in advance. Then the powdered sample of $SrIrO_3$ at 2.0% was added to that of the $Sr_3Ir_2O_7$ to be evaluated. From the magnitude of the enhancement in intensity of the XRD peaks for $SrIrO_3$ in the mixed sample, a value for the fraction of $SrIrO_3$ was estimated to be about 2%.

Estimated lattice parameters, assuming tetragonal structure, are $a = 3.9026$ Å and $c = 20.9300$ Å, which are good agreement with the previous report [21]. The dc magnetization
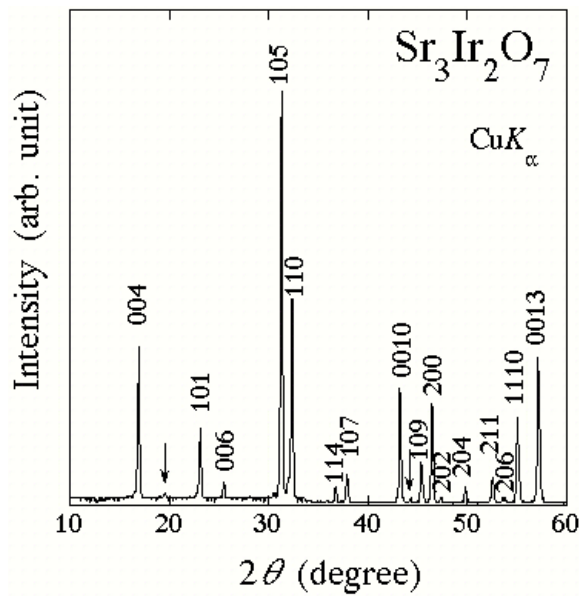
Figure 1. X-ray powder diffraction pattern of the polycrystalline sample of $Sr_3Ir_2O_7$. The arrowed peaks correspond to those of impurity-phase $SrIrO_3$. The fraction was estimated to be $\sim$2%, and the details are described in section 2.

was measured using a superconducting quantum interference detector (SQUID) magnetometer (Quantum Design, MPMS) from 1.8 to 400 K. The contribution of impurity-phase $SrIrO_3$ to the magnetization is negligible, because of the following two reasons: (1) the $SrIrO_3$ fraction is tiny ($\sim$2%), and (2) $SrIrO_3$ shows weak paramagnetism in the temperature dependence of magnetic susceptibility [20], the value of which is 2.7×10^{-4} emu/mol Oe at 300 K, from the preliminary experimental results. The electrical resistivity was measured using a standard four-probe method in the temperature range 50–330 K. The specific heat was measured using the relaxation method (Quantum Design, PPMS) in the temperature range 150–370 K. For transmission electron microscopy (TEM), the specimens were mechanically polished and ion-milled. TEM observations were performed using a JEM-4000FX at an accelerating voltage of 200 kV using an N_2 cooling stage. Parallel beam and convergent beam electron diffraction (CBED) patterns were taken at various crystallographic orientations at 315 and 200 K.

3. Results

Figure 2 displays the temperature dependences of magnetization $M(T)$ per Ir ion for $Sr_3Ir_2O_7$ in a field cooled sequence (FC) and a zero field cooled sequence (ZFC) at a field of $H = 10\,000$ Oe, where FC means that magnetization was measured on cooling at $10\,000$ Oe from 330 K, and ZFC indicates the measurement on heating at $10\,000$ Oe after cooling in the zero magnetic field from 330 to 5 K. It is found that a magnetic transition clearly occurs at $T_C \sim 280$ K. A substantial increase is observed below T_C with a weak ferromagnetic component, indicated by the significant hysteresis between the ZFC and FC sequences. The value of T_C is very close to that of the single-crystalline material [23].

The temperature dependences of magnetic susceptibility, $\chi(T) = M/H$ with $H = 10$ Oe and 1000 Oe in the FC sequence for polycrystalline $Sr_3Ir_2O_7$, also show a substantial increase
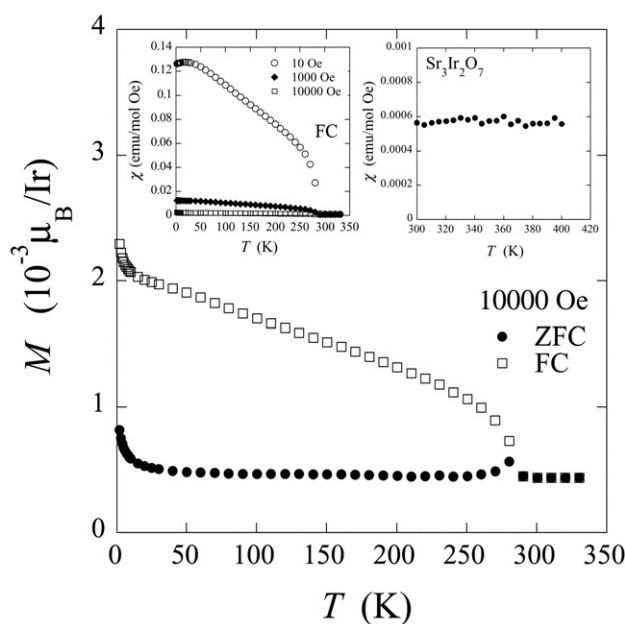
Figure 2. The temperature dependence of magnetization for $Sr_3Ir_2O_7$ in an FC sequence and a ZFC sequence with $H = 10\,000$ Oe. The left inset displays the temperature dependence of susceptibility in an FC sequence with $H = 10$, 1000 and $10\,000$ Oe. The magnetic susceptibility for $Sr_3Ir_2O_7$ in the high-temperature range $300–400\,K > T_c$ with $H = 10\,000$ Oe indicates temperature independence, as shown in the right inset.

below T_C and a positive value down to 5 K, the same as in the case for $H = 10\,000$ Oe, as shown in the left inset. Single-crystalline $Sr_3Ir_2O_7$ grown by a flux method [23] provides strange magnetic properties such that χ for the $H \parallel ab$-plane undergoes a rapid drop below 50 K, and becomes negative below 20 K in the FC sequence, although χ for the $H \parallel c$-axis remains positive down to 1.7 K. The intrinsic magnetic properties of our polycrystalline sample must be different from those of the single-crystalline $Sr_3Ir_2O_7$, even if we take account of the magnetic anisotropy [23]. There are some reports that the magnetism observed in samples of some ruthenates depends on the synthetic method [4–6]. The ferromagnetic component ($2 \times 10^{-3}\ \mu_B/Ir$) at 5 K is much smaller than that expected for $s = 1/2$ of Ir^{4+} with a low spin state. The weak ferromagnetic transition reflects the bulk nature, since the temperature dependence of specific heat exhibits a clear anomaly at T_C, as discussed later. Therefore, these results indicate that a certain magnetic long-range ordering with weak ferromagnetism occurs below $\sim$280 K in $Sr_3Ir_2O_7$. In the temperature range $300–400\,K > T_C$, the magnetic susceptibility is temperature independent, as shown in the right inset. In other words, this does not obey the Curie–Weiss law.

　　Figure 3 shows the magnetization curves (field dependence of magnetization) $M(H)$ for a ZFC sequence in $Sr_3Ir_2O_7$ at various temperatures. The M was measured on increasing magnetic field up to 7 T at each measuring temperature $T_m(= 50, 100, 200, 280, 330\,K)$ after cooling in the zero magnetic field from 330 K to T_m, and then M was measured on decreasing the magnetic field down to 0 T at T_m. The hysteresis has been observed clearly below T_C. The value of the magnetization curves at 1 T is much smaller than that from the temperature dependence of magnetization at 1 T, because the former and the latter sequences for measuring M are different. Below the magnetic transition temperature, any clear metamagnetic
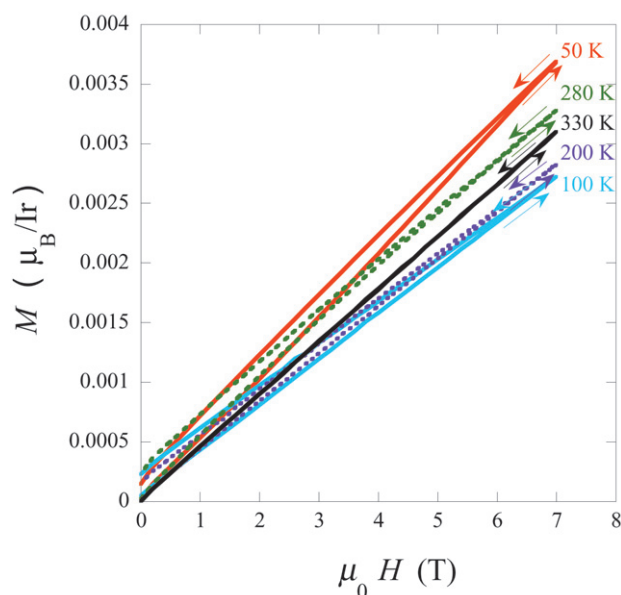
Figure 3. The magnetization curves below or above T_C for $Sr_3Ir_2O_7$.

(This figure is in colour only in the electronic version)

transition has not appeared in the magnetic field range 0–7 T. The magnetizations have not been saturated until 7 T. These facts imply that the observed weak ferromagnetism is not simple ferromagnetism in $Sr_3Ir_2O_7$. On the other hand, no hysteresis has been observed and the magnetization is relative to the magnetic field for $T = 330$ K. This indicates that this compound shows paramagnetism at 330 K, which is consistent with the result for magnetization, as shown in figure 2.

The temperature dependence of electrical resistivity $\rho(T)$ for $Sr_3Ir_2O_7$ is shown in figure 4. No hysteresis has been seen between heating and cooling sequences. The figure indicates $d\rho/dT < 0$ in the temperature range 50–330 K. At least, this non-metallic transport property below 280 K is intrinsic in $Sr_3Ir_2O_7$, because the impurity $SrIrO_3$ included in the $Sr_3Ir_2O_7$ sample shows good metallic behaviour below RT [20]. The value of resistivity at ~300 K for $Sr_3Ir_2O_7$ (250 mΩ cm) is smaller than that of other semiconducting polycrystalline oxides like Sr_2IrO_4 (~7 Ω cm) [18] and Ca_2RuO_4 (~6 Ω cm for the tetragonal phase, ~400 Ω cm for the orthohombic phase) [26]. It has been found that the resistivity increases steeply with decreasing temperature below 280 K, nearly equal to T_c. In contrast, no corresponding anomaly is observed in the resistivity near the ferromagnetic transition temperature $T_C = 240$ K for both single-crystalline Sr_2IrO_4 [16] and polycrystalline Sr_2IrO_4 [15, 17, 18]. The semiconducting behaviour and the electrical anomaly at $T_c \sim 280$ K are also observed in single-crystalline $Sr_3Ir_2O_7$ [23]. Neither the Arrhenius law nor the law expressed by the form $\rho = A \exp(T_0/T)^\alpha$, which is associated with the variable-range hopping of carriers, is capable in the temperature range 2–280 K.

Figure 5 displays the temperature dependence of the specific heat $C(T)$ in zero magnetic field. No hysteresis appears between the heating and cooling sequences, which is the same as the result for the resistivity measurement. This exhibits a λ-type anomaly at $T_c \sim 280$ K, indicating a second-order phase transition. The magnitude of the jump in specific heat at 280 K
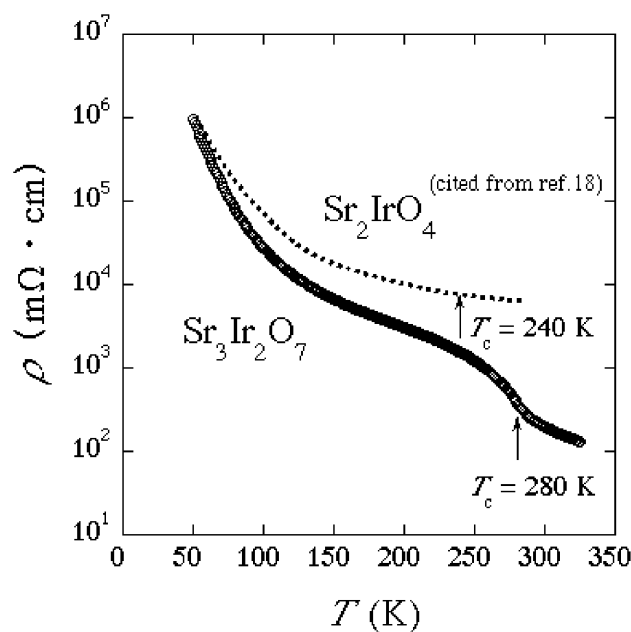
Figure 4. The temperature dependences of electrical resistivity for polycrystalline samples of Sr$_3$Ir$_2$O$_7$.

is sufficiently large such that this anomaly is not derived from an impurity such as SrIrO$_3$. That is to say, this phase transition is essential for Sr$_3$Ir$_2$O$_7$. According to our ED measurements, there is no evidence for a distinct structural phase transition with a symmetry change at 280 K, as discussed later. Taking account of the semiconducting magnetic ordered state below 280 K, the total specific heat is regarded as a summation of the lattice and magnetic contributions below T_c. Here, the magnetic component of specific heat originates from magnons due to the long-range magnetic ordering. No structural transition at T_c indicates that the anomaly should not appear in the lattice specific heat at this temperature. In other words, the observed specific heat anomaly only comes from the magnetic phase transition. Hence, the observed anomaly with a λ-type peak around 280 K evidences the bulk nature of the magnetic long-range ordering in Sr$_3$Ir$_2$O$_7$.

   Figure 6 shows one of the electron diffraction patterns taken in the [001] orientation (a) at 315 K and (b) at 200 K. Weak diffraction spots like 100 and 010 in the figure 6(a) are considered to be due to the multiple diffraction effect. The diffraction pattern shows that the space group is *Bbcb* (*D22/2h*, no. 68 in the International Table for Crystallography) [25]. There are no changes of diffraction spots between 200 and 315 K, which indicates that there is no lattice structural transition at $T_c \sim 280$ K. However, the possibility of change in the rotation angle of octahedrons remains, because such a change does not lead to a drastic deformation. Figure 7 exhibits the convergent beam electron diffraction pattern taken at the [001] zone axis orientation at 315 K. Comparing with the magnitude of intensity of the arrowed peaks, the whole pattern looks like 2*mm* symmetry. This is caused by the micro-twin structure along the [001] zone axis. The twin structure consists of *Bbcb* and *Acaa* domains, whose rotation directions for vertical neighbouring pairs of IrO$_6$ octahedrons are opposite. The difference between *Bbcb* and *Acaa* structures is derived from a difference in the stacking along the *c*-axis. The reason why the pattern shows 2*mm*-like symmetry is that both the *Bbcb* and *Acaa* reciprocal lattices
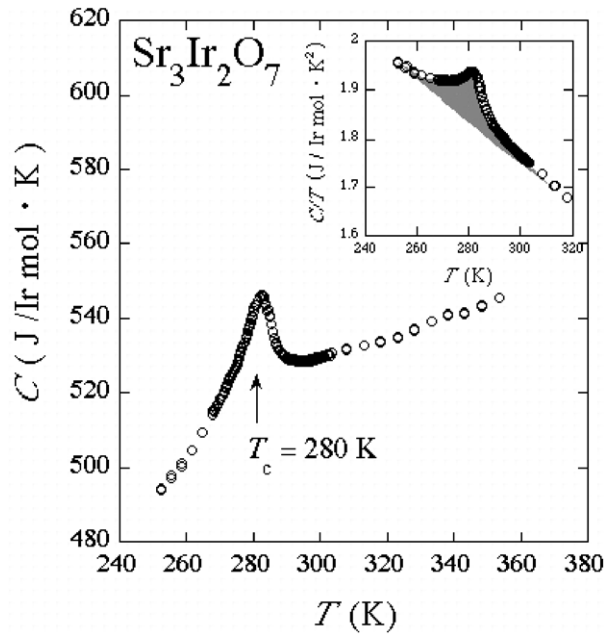
Figure 5. The temperature dependence of the specific heat for $Sr_3Ir_2O_7$ in zero magnetic field. The T versus C/T plot is shown in the inset.

are superimposed. This result is consistent with the previous report on electron diffraction measurements [25].

4. Discussions

We discuss the origin of weak ferromagnetism below $T_C \sim 280$ K in $Sr_3Ir_2O_7$ based on the present experimental results. Considering the specific heat and structural analysis by electron diffraction, there are two possibilities for the nature. One is simple ferromagnetism with a quite small spin moment; the other is canted antiferromagnetism. In general, the total specific heat C is regarded as a summation of a phonon component C_{ph} and a magnetic component C_{mag} for an insulator with magnetic ordering. In a higher temperature range than the Debye temperature, it is impossible to separate C_{mag} and C_{ph} clearly because $C_{ph} \gg C_{mag}$. Therefore, it is difficult to estimate the experimental value of the transition entropy $S_{mag(ex)}$ which is associated with this magnetic transition at T_C in $Sr_3Ir_2O_7$. In order to confirm whether the weak ferromagnetism is derived from the former case or the latter case, we try to estimate the value of the lower limit of transition entropy, $S^L_{mag(ex)}$, associated with this magnetic transition at T_C. The value of $S^L_{mag(ex)}$ should be equal to the area of the specific heat jump, which is represented as the shadow area in the inset of figure 5. The obtained value of $S^L_{mag(ex)}$ is 1.7 J/Ir mol K. If the Ir^{4+} spins are ordered ferromagnetically below T_C, Ir^{4+} ion should have a quite small spin moment, $s = 1 \times 10^{-3}$, associated with the ferromagnetic component $2 \times 10^{-3} \mu_B$/Ir obtained from the temperature dependence of magnetization. The theoretical value of $S_{mag(th)}$ is estimated by the following equation, assuming simple ferromagnetism: $S_{mag(th)} = N k_B \ln(2s+1)$, where N is Avogadro's number. When the value of 1×10^{-3} is substituted for s in this equation, the value of $S_{mag(th)}$ is 0.02 J/Ir mol K. If the observed weak ferromagnetism is simple ferromagnetism with such
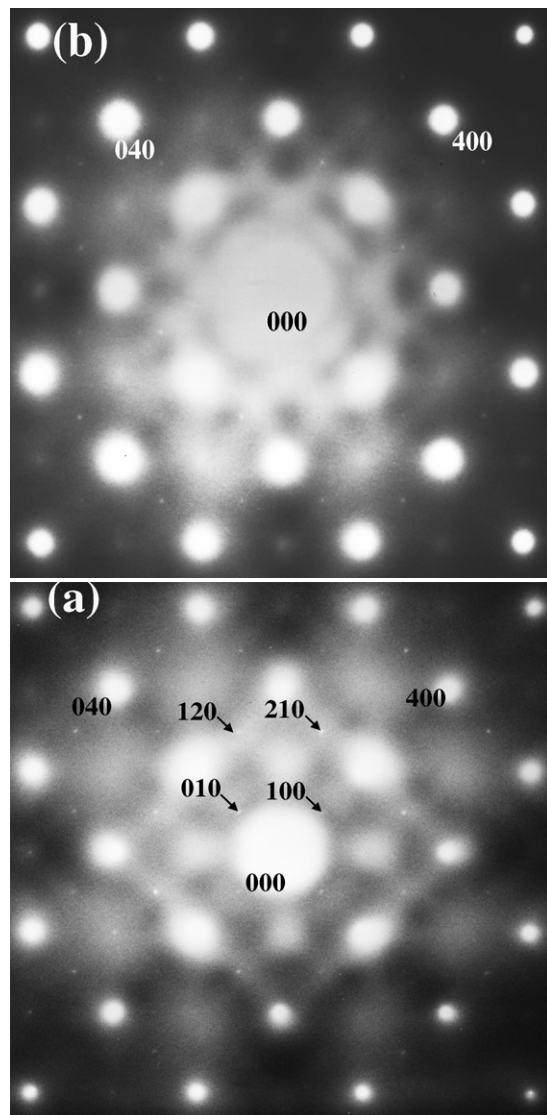
Figure 6. The electron diffraction pattern taken at the [001] orientation (a) at 315 K and (b) at 200 K.

a small spin moment, the estimated value of $S_{mag(ex)}$ should be approximately 0.02 J/Ir mol K. However, the value of $S_{mag(ex)}^{L}$ is 85 times larger than the value of $S_{mag(th)}$. This indicates that the possibility of simple ferromagnetism with a quite small spin moment is excluded as the origin of the weak ferromagnetism.

The appearance of canted antiferromagnetism also depends on whether certain pairs of Ir^{4+} ions lose the centre of inversion or not. According to a previous report on structural Reitveld analysis using single-crystalline $Sr_3Ir_2O_7$, it has been confirmed that IrO_6 octahedral rotations exist within the IrO_2 plane in $Sr_3Ir_2O_7$ [21]. In this case, certain pairs of Ir^{4+} ions lose the centre of inversion, leading to the Dzyaloshinsky–Moriya (DM) interaction between Ir^{4+} ions inducing the canted antiferromagnetism with weak ferromagnetism when the interaction
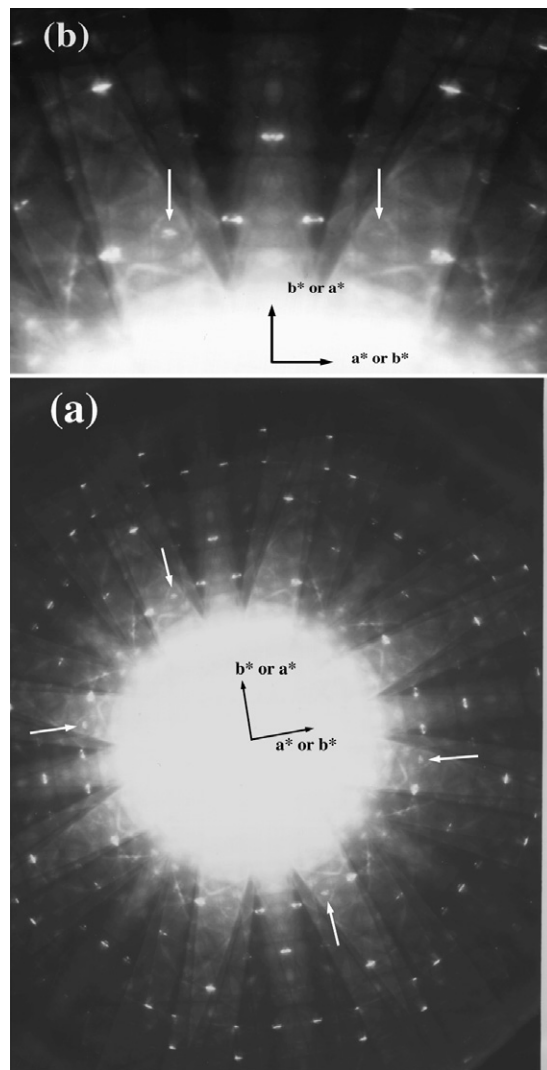
Figure 7. The convergent beam electron diffraction pattern taken at the [001] zone axis orientation at 315 K. (b) An expanded figure of the upper region of (a). Magnitudes of intensities of the four arrowed spots are similar in (a), whereas those of the two arrowed spots are different in (b).

between the spin pairs is antiferromagnetic. Therefore, the weak ferromagnetism can be explained quite naturally as being due to the DM interaction in $Sr_3Ir_2O_7$. Considering the magnetizations as shown in figure 3, it is suggested that the metamagnetic transition associated with spin-flip appears above 7 T.

These results drive us to the question whether $Sr_3Ir_2O_7$ is a Mott insulator or not. Although the temperature dependence of resistivity exhibits semiconducting-like behaviour even above T_C, it is not clear that this indicates the existence of a gap at the Fermi level in the density of states beyond T_C. $Sr_3Ir_2O_7$ can be a Mott insulator if various transport properties show insulating features above T_C intrinsically. For this purpose, other experiments, e.g. thermoelectric power and optical conductivity, should be performed.

5. Conclusions

The magnetic, transport and structural properties of a polycrystalline $Sr_3Ir_2O_7$ prepared by a high-pressure synthesis technique have been investigated. Weak ferromagnetism with a small ferromagnetic component (2×10^{-3} μ_B/Ir) was observed below $T_C \sim 280$ K. We confirm that the weak ferromagnetism below T_C is derived from the bulk nature of $Sr_3Ir_2O_7$. Moreover, it has been found that this ferromagnetism can be explained quite naturally as being due to the Dzyaloshinsky–Moriya interaction, which leads to canted antiferromagnetism.

Acknowledgments

References

[1] Bednorz J G and Muller K A 1986 *Z. Phys.* **64** 189
[2] Huang Q, Lynn J W, Erwin R W, Jarupatrakorn J and Cava R J 1998 *Phys. Rev.* B **58** 8515
[3] Shaked H, Jorgensen J D, Chmaissen O, Ikeda S and Maeno Y 2000 *J. Solid State Chem.* **154** 361
[4] Cava R J, Zandbergen H W, Krajewski J J, Peck W F, Batlogg B, Carter S, Fleming R M, Zhou O and Rupp L W 1995 *J. Solid State Chem.* **116** 141
[5] Ikeda S I, Maeno Y and Fujita T 1998 *Phys. Rev.* B **57** 978
[6] Cao G, McCall S and Crow J E 1997 *Phys. Rev.* B **55** R672
[7] Ikeda S I and Maeno Y 1999 *Physica* B **259–261** 947
[8] Ikeda S I, Maeno Y, Nakatsuji S, Kosaka M and Uwatoko Y 2000 *Phys. Rev.* B **62** R6089
[9] Hase I and Nishihara Y 1997 *J. Phys. Soc. Japan* **66** 3517
[10] Perry R S, Galvin L M, Grigera S A, Capogna L, Schofield A J, Mackenzie A P, Chiao M, Julian S R, Ikeda S I, Nakatsuji S, Maeno Y and Pfleiderer C 2001 *Phys. Rev. Lett.* **86** 2661
[11] Grigera S A, Perry R S, Schofield A J, Chiao M, Julian S R, Lonzarich G G, Ikeda S I, Maeno Y, Millis A J and Mackenzie A P 2001 *Science* **294** 329
[12] Ikeda S I, Azuma U, Shirakawa N, Nishihara Y and Maeno Y 2002 *J. Cryst. Growth* **237** 787
[13] Capogna L, Forgan E M, Hayden S M, Wildes A, Duffy J A, Mackenzie A P, Perry R S, Ikeda S I, Maeno Y and Brown S P 2003 *Phys. Rev.* B **67** 012504
[14] Maeno Y, Hashimoto H, Yoshida K, Nishizaki S, Fujita T, Bednortz J G and Lichtenberg F 1994 *Nature* **372** 532
[15] Crawford M K, Shubramanian M A, Harlow R L, Fernandez-Baca J A, Wang Z R and Johnston D C 1994 *Phys. Rev.* B **49** 9198
[16] Cao G, Bolivar J, McCall S, Crow J E and Guertin R P 1998 *Phys. Rev.* B **57** R11039
[17] Shimura T, Inaguma Y, Nakamura T, Itou M and Morii Y 1995 *Phys. Rev.* B **52** 9143
[18] Cava R J, Batlogg B, Kiyono K, Takagi H, Krajewski J J, Peck W F, Rupp L W and Chen C H 1994 *Phys. Rev.* B **49** 11890
[19] Huang Q, Soubeyroux J L, Chmaissem O, Natali Sora I, Santoro A, Cava R J, Krajewski J J and Peck W F 1994 *J. Solid State Chem.* **112** 355
[20] Longo J M, Kafalas J A and Arnott R J 1971 *J. Solid State Chem.* **3** 174
[21] Shubramanian M A, Crawford M K and Harlow R L 1994 *Mater. Res. Bull.* **29** 645
[22] Kafalas J A and Longo J M 1972 *J. Solid State Chem.* **4** 55
[23] Cao G, Xin Y, Alexander C S, Crow J E, Schlottmann P, Crawford M K, Harlow R L and Marshall W 2002 *Phys. Rev.* B **66** 214412
[24] Nagai I, Ikeda S I, Yoshida Y, Kito H and Shirakawa N 2003 *J. Low Temp. Phys.* **131** 665
[25] Matsuhata H, Nagai I, Yoshida Y, Hara S, Ikeda S I and Shirakawa N 2004 *J. Solid State Chem.* **177** 3776
[26] Nakatsuji S, Ikeda S I and Maeno Y 1997 *J. Phys. Soc. Japan* **66** 1868